

## Polyallene with pendant nitroxyl radicals

Xiaohuan Zhang<sup>a</sup>, Huiqiao Li<sup>b</sup>, Litao Li<sup>a</sup>, Guolin Lu<sup>a</sup>, Sen Zhang<sup>a</sup>, Lina Gu<sup>a</sup>, Yongyao Xia<sup>b,\*</sup>, Xiaoyu Huang<sup>a,\*\*</sup>

<sup>a</sup> Laboratory of Polymer Materials and Key Laboratory of Organofluorine Chemistry, Shanghai Institute of Organic Chemistry, Chinese Academy of Sciences, 354 Fenglin Road, Shanghai 200032, PR China

<sup>b</sup> Department of Chemistry and Shanghai Key Laboratory of Molecular Catalysis and Innovative Materials, Fudan University, 220 Handan Road, Shanghai 200433, PR China

### ARTICLE INFO

#### Article history:

Received 9 May 2008

Received in revised form 6 June 2008

Accepted 6 June 2008

Available online 18 June 2008

#### Keywords:

Polyallene

Synthesis

Polyradical

### ABSTRACT

A new polyradical containing polyallene backbone and stable pendant nitroxyl radicals was synthesized using 4-hydroxyl-2,2,6,6-tetramethylpiperidine as starting material. Firstly, a new allenyl ether monomer, 4-allenyloxy-2,2,6,6-tetramethyl piperidine was prepared by 2 steps. Next, BPO initiated the traditional free radical polymerization of 4-allenyloxy-2,2,6,6-tetramethyl piperidine at 100 °C to obtain the homopolymer, poly(4-allenyloxy-2,2,6,6-tetramethyl piperidine). Finally, the homopolymer was quantitatively oxidized by H<sub>2</sub>O<sub>2</sub>/Na<sub>2</sub>WO<sub>4</sub>·2H<sub>2</sub>O/EDTA at room temperature to yield the final product, poly(4-allenyloxy-2,2,6,6-tetramethyl piperidine-1-oxyl). Studies on the electrochemical properties of polyradical showed excellent charging/discharging reversibility and stability with a high columbic efficiency of 98%, which suggested that the synthesized polyradical is a promising cathode material for lithium secondary battery.

© 2008 Elsevier Ltd. All rights reserved.

### 1. Introduction

Recently, polyradical has been paid much attention due to its specific characteristics which originate from the paramagnetism and it has been applied in many fields. For example, polyradical can be used as one-dimensional throw-bond organic ferromagnets [1,2]. Also, it was found that many polyradicals can be oxidized and reduced electrochemically [3,4]. Polymeric nitroxyl radical with bulky substituents is usually employed as efficient mediator for the selective oxidations of primary, secondary mono-alcohols, diols and polyols [3,5–8].

Especially, many kinds of stable polymeric nitroxyl radicals can be used as cathode material due to their high electrochemical stability and rapid charging/discharging ability in the energy storage system [9–13] and they are under development for use in bendable electronic equipment [14]. The charging and discharging mechanisms were proved be a redox process so that polymeric nitroxyl radicals did not produce single anionic and cationic radical during the process, which kept the chemical structure of polymeric nitroxyl radicals when charging and discharging. Their physico-chemical properties can be modified by adjusting the composition and the structure, blending and copolymerization [15]. Thus,

polyradical can be expected to be developed as a new material of energy storage. Generally, 2 approaches are employed for the synthesis of polymeric nitroxyl radicals. One is to synthesize the monomer consisting of radical followed by the polymerization [16]; the other is to oxidize the prepolymer. Since the nitroxyl radical is a kind of radical trap, the second method is more applicable [17].

It is well known that allene derivatives have cumulated double bonds. They can be regarded as the isomers of propargyl ether derivatives. Due to this structure characteristic, if either part (1,2- or 2,3) of the cumulated double bonds can be selectively polymerized, the obtained polymer (polyallene) possesses non-conjugated double bonds directly linked to the backbone. Thus, the synthesis of allene monomers with a wide variety of functional groups may indicate the potent applicability of polyallene. Also, they can be used as novel reactive polymers as well as functional materials due to the versatility of the addition reactions of the double bonds [18]. In comparison with polymeric nitroxyl radicals, polyallene is more unsaturated due to the attached double bonds, which was expected to benefit the transport of the electron.

Allene derivatives can be polymerized by many different methods including the radical, cationic, coordination and zwitterionic polymerizations [19]. In particular, allenyl ether monomers can be polymerized by traditional free radical polymerization using benzoyl peroxide (BPO) as initiator and they can be easily prepared by the isomerization of propargyl ether.

In this work, we report the synthesis of a new polyallene-based polyradical containing stable pendant nitroxyl radicals.

\* Corresponding author. Tel.: +86 21 55664397; fax: +86 21 55664177.

\*\* Corresponding author. Tel.: +86 21 54925310; fax: +86 21 64166128.

E-mail addresses: [yyxia@fudan.edu.cn](mailto:yyxia@fudan.edu.cn) (Y. Xia), [xyhuang@mail.sioc.ac.cn](mailto:xyhuang@mail.sioc.ac.cn) (X. Huang).

4-Hydroxyl-2,2,6,6-tetramethylpiperidine (HTMP) was used as starting material to synthesize the target monomer, 4-allenyloxy-2,2,6,6-tetramethyl piperidine (ATMP) by 2 steps. Next, ATMP was initiated by BPO for traditional free radical polymerization at 100 °C to obtain the homopolymer, poly(4-allenyloxy-2,2,6,6-tetramethyl piperidine) (PATMP). Finally, PATMP was oxidized by H<sub>2</sub>O<sub>2</sub>/Na<sub>2</sub>WO<sub>4</sub>·2H<sub>2</sub>O/EDTA in methanol at room temperature to yield the final product, poly(4-allenyloxy-2,2,6,6-tetramethyl piperidine-1-oxyl) (PATMPO) as shown in Scheme 1. Electrochemical properties of PATMPO polyradical were also preliminarily studied.

## 2. Experimental section

### 2.1. Materials

Benzoyl peroxide (BPO, Aldrich, 97%) was recrystallized from chloroform and methanol at room temperature. 2,2'-Azobis(isobutyronitrile) (AIBN, Aldrich, 98%) was recrystallized from anhydrous ethanol. Tetrahydrofuran (THF) was dried over CaH<sub>2</sub> for 1 week and distilled from sodium and benzophenone under N<sub>2</sub> prior to use. 4-Hydroxyl-2,2,6,6-tetramethylpiperidine (HTMP, TCI, 95%), sodium hydride (NaH, Aldrich, 60% dispersion in mineral oil), potassium *tert*-butoxide (tBuOK, Aldrich, 95%), propargyl bromide (TCI, 97%), hydrogen peroxide (H<sub>2</sub>O<sub>2</sub>, Aldrich, 35% in water), ethylenediaminetetraacetic acid (EDTA, Aldrich, 99.95%), *tert*-butyl alcohol (Alfa Aesar, 99.8%) and sodium tungstate dihydrate (Na<sub>2</sub>WO<sub>4</sub>·2H<sub>2</sub>O, Aldrich, 99%) were used as-received.

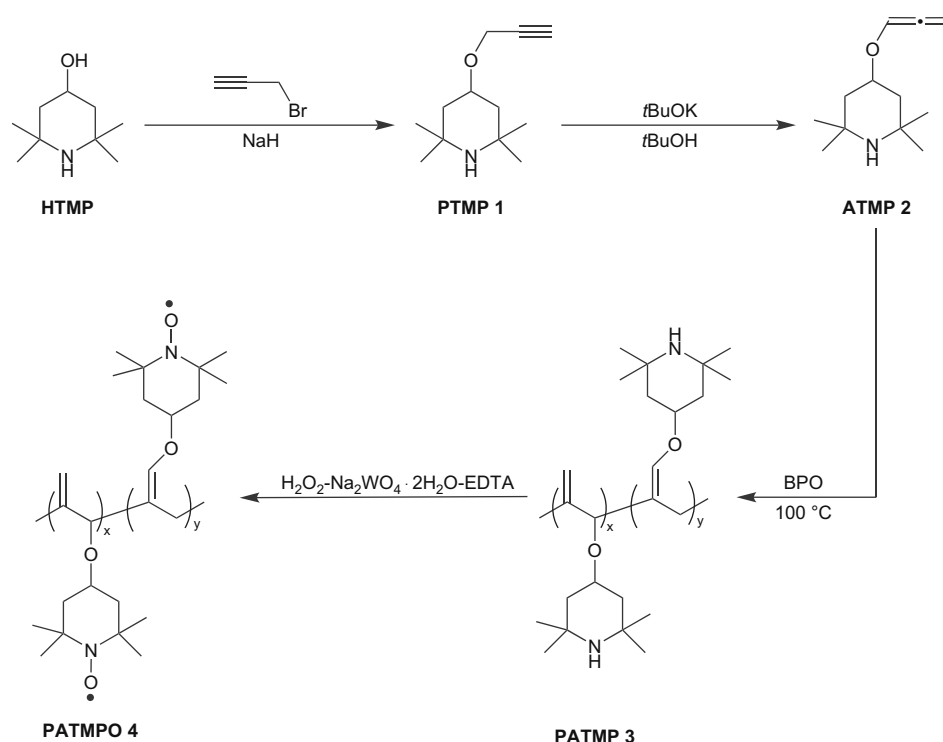
### 2.2. Measurements

FT-IR spectra were recorded on a Nicolet AVATAR-360 FT-IR spectrophotometer with 4 cm<sup>-1</sup> resolution. UV-vis spectra were measured by a Cary-100 Bio UV-vis spectrometer. Elemental analysis was carried out on a Carlo-Erba 1106 system. Relative molecular weights and molecular weight distributions were determined by gel permeation chromatography (GPC) system

equipped with a Waters 1515 Isocratic HPLC pump, a Waters 2414 refractive index detector (RI) and a set of Waters Styragel columns (HR3, HR4 and HR5, 7.8 × 300 mm). GPC measurements were carried out at 35 °C using THF as eluent with a 1.0 mL/min flow rate. The system was calibrated with polystyrene standards. All NMR analyses were performed on a Bruker Avance 500 spectrometer (500 MHz) in CDCl<sub>3</sub>; TMS (<sup>1</sup>H NMR) and CDCl<sub>3</sub> (<sup>13</sup>C NMR) were used as the internal standards. Electron spin resonance (ESR) was measured by a Bruker EMX-8/2.7 spectrometer. Charging–discharging experiments were carried out on a Land BS-9300 battery charge–discharge instrument at room temperature. To prepare the electrode, a usual mixture of 10% polyradical, 80% conductive graphite and 10% poly(tetrafluoroethylene) (PTFE) binder was homogeneously dispersed in isopropanol with stirring. The resulting clay was pressed onto an Al grid collector and then dried at 80 °C for 12 h *in vacuo*. The coin-type cell was fabricated by stacking polyradical electrode, separator and lithium in a glove box under Ar. The electrolyte was 1 M LiPF<sub>6</sub> in ethylene carbonate (EC)/dimethyl carbonate (DMC) solution (v/v = 1:2).

### 2.3. Preparation of 4-propargyloxy-2,2,6,6-tetramethyl piperidine

4-Hydroxyl-2,2,6,6-tetramethylpiperidine (40.0 g, 0.255 mol) was firstly dissolved in 400 mL of dry THF followed by adding NaH (6.74 g, 0.280 mol) slowly. Next, the mixture was refluxed for 3 h and then cooled to room temperature. Propargyl bromide (30.3 g, 0.255 mol) was added dropwise and the mixture reacted overnight. The reaction was quenched by adding water and the solution was washed with brine and dried over anhydrous MgSO<sub>4</sub>. After concentration, crude product was separated at –18 °C. White needle crystal (20.3 g, 40.8% yield), 4-propargyloxy-2,2,6,6-tetramethyl piperidine (PTMP **1**), was obtained after washing with cold *n*-hexane. FT-IR:  $\nu$  (KBr, cm<sup>-1</sup>): 3309, 2957, 2929, 2112, 1728, 1457, 1377, 1366, 1312, 1236, 1189, 1165, 1084, 1015, 965, 912, 799, 662. <sup>1</sup>H NMR (500 MHz, CDCl<sub>3</sub>):  $\delta$  (ppm): 1.02, 1.97 (4H, CH<sub>2</sub> of piperidine), 1.15 (12H, CH<sub>3</sub> of piperidine), 2.41 (1H, OCH<sub>2</sub>C≡CH), 3.94 (1H, CH of piperidine), 4.21



Scheme 1. Synthesis of polyallene with pendant nitroxyl radicals.

(2H,  $\text{OCH}_2\text{C}\equiv\text{CH}$ ).  $^{13}\text{C}$  NMR (125 MHz,  $\text{CDCl}_3$ ):  $\delta$  (ppm): 28.8, 34.8, 44.3, 51.4, 54.7, 71.7, 73.8, 80.1. Anal. Calcd. for  $\text{C}_{12}\text{H}_{21}\text{NO}$ : C, 73.80; H, 10.84; N, 7.17. Found: C, 73.63; H, 11.23; N, 6.89.

#### 2.4. Preparation of 4-allenyloxy-2,2,6,6-tetramethyl piperidine

PTMP **1** (20.3 g, 0.10 mol) and *t*BuOK (11.7 g, 0.10 mol) were added to 300 mL of *tert*-butyl alcohol and the solution was refluxed for 3 h. The reaction mixture was poured into water and extracted with ether. The extract was washed with water to remove residual *tert*-butyl alcohol and dried over  $\text{MgSO}_4$  followed by concentration. A yellowish liquid, ATMP **2** (11.8 g, 58.1% yield), was obtained by neutral alumina column chromatography using *n*-hexane/ether (14:3 v/v) as eluent. FT-IR:  $\nu$  (KBr,  $\text{cm}^{-1}$ ): 3311, 3037, 2956, 2928, 2855, 1951, 1458, 1445, 1377, 1365, 1348, 1308, 1236, 1195, 1036, 887, 856, 697.  $^1\text{H}$  NMR (500 MHz,  $\text{CDCl}_3$ ):  $\delta$  (ppm): 0.82, 1.95 (2H,  $\text{CH}_2$  of piperidine), 1.13 (6H,  $\text{CH}_3$  of piperidine), 4.05 (1H,  $\text{CH}$  of piperidine), 5.35 (2H,  $-\text{OCH}=\text{C}=\text{CH}_2$ ), 6.59 (1H,  $-\text{OCH}=\text{C}=\text{CH}_2$ ).  $^{13}\text{C}$  NMR (125 MHz,  $\text{CDCl}_3$ ):  $\delta$  (ppm): 28.8, 34.8, 44.2, 51.6, 71.9, 89.8, 119.8, 201.5. Anal. Calcd. for  $\text{C}_{12}\text{H}_{21}\text{NO}$ : C, 73.80; H, 10.84; N, 7.17. Found: C, 73.67; H, 10.55; N, 6.94.

#### 2.5. Homopolymerization of ATMP

In a typical procedure, a 25 mL dried Schlenk flask was charged with BPO (14.7 mg, 0.061 mmol) under  $\text{N}_2$ . Next, ATMP **2** (11.8 g, 60.5 mmol) was introduced via a gastight syringe. The flask was degassed by 3 cycles of freezing–pumping–thawing followed by immersing the flask into an oil bath thermostated at 100 °C. After 35 h, the polymerization was terminated by putting the flask into liquid nitrogen. The reaction mixture was diluted by THF and precipitated into cold *n*-hexane. The product was dried *in vacuo* to give 2.11 g of poly(4-allenyloxy-2,2,6,6-tetramethyl piperidine) (PATMP **3**) with a yield of 19.8%. GPC:  $M_n = 1.98 \times 10^4$  g/mol,  $M_w/M_n = 1.82$ . FT-IR:  $\nu$  (KBr,  $\text{cm}^{-1}$ ): 3318, 2957, 2927, 2128, 1687, 1630, 1545, 1479, 1457, 1435, 1377, 1365, 1234, 1190, 1168, 1076, 1016, 989, 909, 805, 733, 642.  $^1\text{H}$  NMR (500 MHz,  $\text{CDCl}_3$ ):  $\delta$  (ppm): 1.16 (12H,  $\text{CH}_3$  of piperidine), 1.77, 1.93 (4H,  $\text{CH}_2$  of piperidine), 2.41, 2.83 (4H,  $=\text{C}-\text{CH}_2-\text{C}=\text{O}$  of the backbone), 3.73, 4.02 (1H,  $\text{CH}$  of the backbone), 4.33 (1H,  $\text{CH}$  of the backbone), 4.88 (2H,  $>\text{C}=\text{CH}_2$  of the backbone), 6.12 (1H,  $-\text{CH}=\text{C}<$  of the backbone), 7.08 (1H,  $\text{NH}$  of piperidine).  $^{13}\text{C}$  NMR (125 MHz,  $\text{CDCl}_3$ ):  $\delta$  (ppm): 29.3, 34.9, 45.1, 68.8, 75.3, 111.0, 115.3, 140.3, 145.4, 147.2. Anal. Calcd. for  $\text{C}_{12}\text{H}_{21}\text{NO}$  repeating unit: C, 73.80; H, 10.84; N, 7.17. Found: C, 72.71; H, 11.45; N, 6.79.

#### 2.6. Oxidation of PATMP

To a 25 mL flask containing PATMP **3** ( $M_n = 1.98 \times 10^4$  g/mol, 1.00 g, 5.1 mmol repeating unit), EDTA (12.9 mg, 0.0442 mmol), sodium tungstate dihydrate (10 mg, 0.0302 mmol) and methanol (6 mL) were added. Next, distilled water (1.06 mL) and  $\text{H}_2\text{O}_2$  (1.06 mL) were added. The product precipitated during the reaction. The reaction lasted for 40 h at room temperature and the orange precipitate was dissolved in THF and precipitated into cold *n*-hexane. Orange powder (0.91 g), PATMPO **4**, was obtained after drying *in vacuo*. GPC:  $M_n = 2.20 \times 10^4$  g/mol,  $M_w/M_n = 1.92$ . FT-IR:  $\nu$  (KBr,  $\text{cm}^{-1}$ ): 2974, 2939, 1749, 1633, 1556, 1463, 1378, 1364, 1242, 1159, 1079, 989, 902, 719. Anal. Calcd. for  $\text{C}_{12}\text{H}_{20}\text{NO}_2$  repeating unit: C, 68.54; H, 9.59; N, 6.66; Found: C, 67.55; H, 10.03; N, 6.01.

### 3. Results and discussion

#### 3.1. Synthesis of allenyl ether monomer

The allenyl ether monomer, 4-allenyloxy-2,2,6,6-tetramethyl piperidine, was prepared by 2 steps using HTMP as starting

material. Firstly, HTMP reacted with propargyl bromide in the presence of NaH (1.1 equiv to hydroxyl group) to provide the intermediate product, PTMP **1**. In particular, the possibility of the formation of *N*-alkylated by-product can be excluded by the absence of the peaks of the protons of the propargyl adjacent to *N*-atom in  $^1\text{H}$  NMR spectrum of PTMP **1** and the good match-up of the result of element analysis with the theoretical value.

Next, ATMP **2** monomer was obtained by the isomerization of PTMP **1** in the presence of potassium *tert*-butoxide [20]. The product was characterized by FT-IR,  $^1\text{H}$  NMR and  $^{13}\text{C}$  NMR. The peak of end double bond appeared at  $887\text{ cm}^{-1}$  in FT-IR spectrum. Fig. 1 shows  $^1\text{H}$  NMR spectrum of ATMP **2**; the signals of 3 protons of allenyl group were found to appear at 5.35 and 6.59 ppm. The peaks at 0.82, 1.13, 1.95 and 4.05 ppm belong to the protons of piperidine, respectively. In addition, the signals at 89.8, 119.8 and 201.5 ppm in  $^{13}\text{C}$  NMR spectrum corresponded to the carbons of  $\text{CH}_2=\text{C}=\text{CH}$ -group, respectively.

Combined with the result of element analysis, all the evidences confirmed the structure of ATMP **2** monomer.

#### 3.2. Synthesis of PATMP

Traditional radical homopolymerization of 4-allenyloxy-2,2,6,6-tetramethyl piperidine was initiated by BPO or AIBN in bulk or solution. The results are summarized in Table 1.

It can be found from Table 1 that homopolymerization of ATMP was obviously affected by the polymerization condition. If the polymerization was run in solution with toluene as solvent, ATMP did not polymerize whenever AIBN or BPO was used as initiator due to the low activity of allyl radical [21] and low concentration of ATMP. However, ATMP can be initiated by BPO in bulk (higher

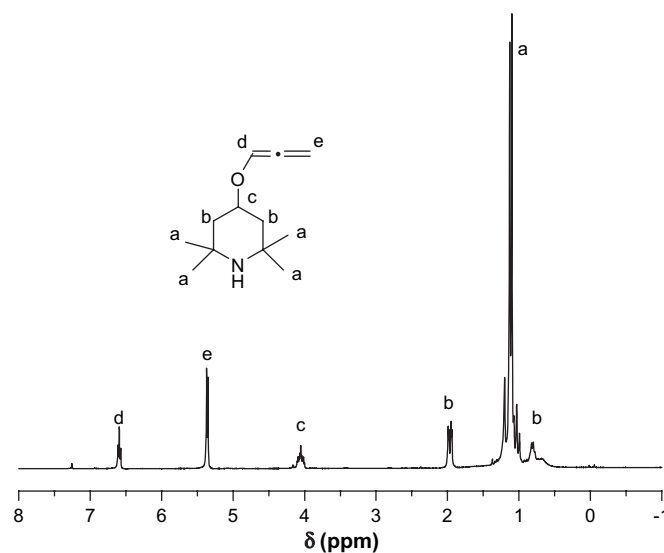


Fig. 1.  $^1\text{H}$  NMR spectrum of ATMP **2** in  $\text{CDCl}_3$ .

Table 1  
Radical homopolymerization of ATMP

Entry	Initiator	[Ini]/[M]	T (°C)	Solvent	Time (h)	$M_n^a$ (g/mol)	$M_w/M_n^a$	Yield (%)
1	AIBN	0.5%	70	Toluene	67	–	–	–
2	BPO	4%	100	Toluene	22	<1300	–	Trace
3	BPO	2%	100	–	10.5	$1.60 \times 10^4$	2.06	34.2
4	BPO	2%	100	–	14.5	$2.40 \times 10^4$	1.64	18.4
5	BPO	0.3%	100	–	24	$9.9 \times 10^3$	1.77	25.5
6	BPO	0.15%	100	–	16.5	$2.04 \times 10^4$	1.68	27.4
7	BPO	0.11%	100	–	35	$1.98 \times 10^4$	1.82	19.8

<sup>a</sup> Measured by GPC in THF at 35 °C.

concentration of ATMP) at 100 °C to obtain PATMP **3** with high molecular weight.

PATMP **3** homopolymer was characterized by FT-IR,  $^1\text{H}$  NMR and  $^{13}\text{C}$  NMR. FT-IR spectrum of PATMP **3** is shown in Fig. 2A. The peaks at 3318 and 1630  $\text{cm}^{-1}$  belong to the imino group of piperidine and the double bond of the backbone, respectively. Two sharp peaks were found to appear at 1365 and 1377  $\text{cm}^{-1}$ , which are attributed to the characteristic signals of gemdimethyl of piperidine. The intensities of both peaks are very close.

Fig. 3 shows  $^1\text{H}$  NMR spectrum of PATMP **3** homopolymer. The signals of the corresponding protons of both piperidine and polyallene backbone can be found. The peaks at 7.08 and 1.16 ppm were attributed to 1 proton of imino group and 12 protons of gemdimethyl of piperidine. The signals of the protons of double bond of polyallene backbone appeared at 4.88 and 6.12 ppm, which indicated that PATMP **3** consisted of both 1,2- and 2,3-polymerized units (labeled as *y* and *x* in Scheme 1). The ratio of 1,2-polymerized units to 2,3-polymerized units was calculated from the integration area ratio of the peak at 6.12 ppm to the peak at 4.88 ppm. The result is 1:2, which means that PATMP **3** homopolymer contained 50% 1,2-polymerized units and 50% 2,3-polymerized units.

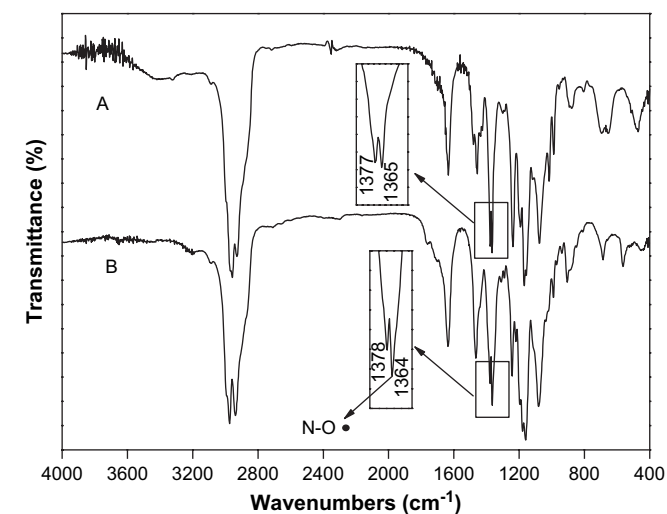


Fig. 2. FT-IR spectra of PATMP **3** (A) and PATMPO **4** (B).

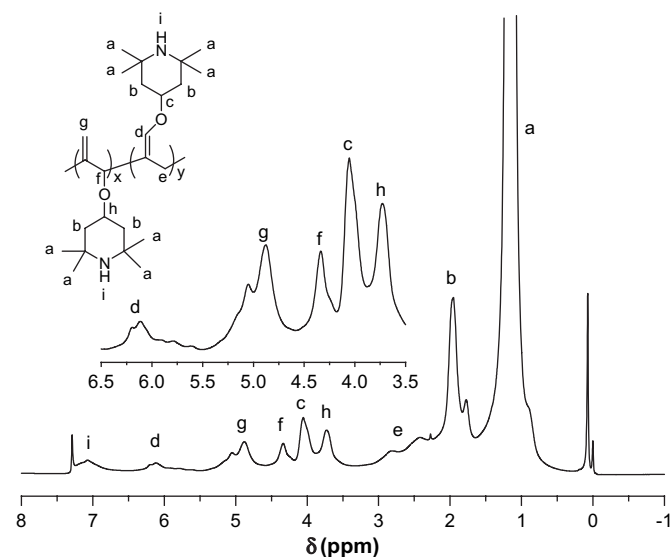


Fig. 3.  $^1\text{H}$  NMR spectrum of PATMP **3** in  $\text{CDCl}_3$ .

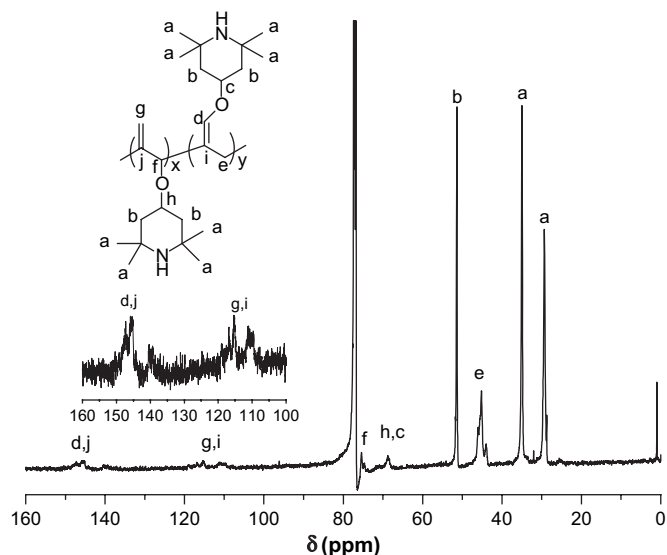


Fig. 4.  $^{13}\text{C}$  NMR spectrum of PATMP **3** in  $\text{CDCl}_3$ .

The signals of the carbons of double bond of polyallene backbone appeared at 111.0, 115.3, 140.3, 145.4 and 147.3 ppm in  $^{13}\text{C}$  NMR spectrum as shown in Fig. 4. The sharp peaks at 29.3 and 34.9 ppm belong to the carbons of gemdimethyl. Thus, all the above results confirmed the successful synthesis of PATMP **3** homopolymer.

### 3.3. Preparation of polyradical

Generally, several methods, including using hydrogen peroxide, lead(IV) oxide, and various peracids, can be employed for the oxidation of imino group to obtain stable nitroxyl radical [22,23]. Among these methods, the pathway using  $\text{H}_2\text{O}_2$  in the presence of sodium tungstate and EDTA is more promising due to its mild reaction condition, high efficiency of oxidation and simple one-step chemical treatment [16]. In our case, we chose this approach to oxidize PATMP **3** homopolymer for preparing polyallene with stable pendant nitroxyl radical, poly(4-allyloxy-2,2,6,6-tetramethyl piperidine-1-oxyl).

FT-IR spectrum after oxidation is shown in Fig. 2B. The intensity of the peak at 1364  $\text{cm}^{-1}$  is obviously higher than that of 1377  $\text{cm}^{-1}$ , which is much different from the case before oxidation as shown in Fig. 2A. This phenomenon demonstrates the formation of nitroxyl radical [16,17], whose peak overlapped with that of gemdimethyl. In addition, the peak of double bond still appeared at 1633  $\text{cm}^{-1}$ , which illustrated that double bond of polyallene backbone was kept during the oxidation.

In comparison with UV–vis spectrum of PATMP **3** as shown in Fig. 5, a new absorption peak appeared at 454 nm associated with an orange color in UV–vis spectrum of PATMPO **4**, which originated from  $n \rightarrow \pi^*$  transition [17]. This result verified the formation of nitroxyl radical. Also, ESR spectrum of PATMPO **4** confirmed the spin species due to the formation of nitroxyl radical.

As reported in previous literature [17], elemental analyses of PATMP **3** and PATMPO **4** were measured to determine whether PATMP **3** was completely oxidized into PATMPO **4** (Table 2). All the measured contents of carbon, hydrogen and nitrogen are in good agreement with the calculated values, which meant that PATMP **3** was oxidized into nitroxyl radical quantitatively.  $M_n$  of PATMPO **4** ( $2.20 \times 10^4$ ) is slightly higher than that of PATMP **3** ( $1.98 \times 10^4$ ) due to the higher molecular weight of repeating units and their molecular weight distributions are very close, which showed that the oxidation process did not destroy the structure of the polymer.

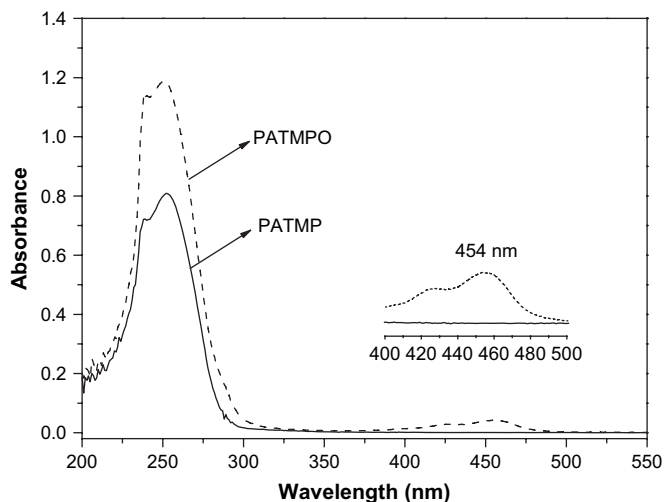


Fig. 5. UV-vis spectra of PATMP **3** and PATMPO **4** in THF.

**Table 2**  
Elemental analysis of PATMP **3** and PATMPO **4**<sup>a</sup>

Element	PATMP <b>3</b>		PATMPO <b>4</b>	
	Calcd.	Found	Calcd.	Found
C	73.85	72.71	68.54	67.55
H	10.77	11.45	9.59	10.03
N	7.18	6.79	6.66	6.01

<sup>a</sup> PATMPO **4** was made from PATMP **3** (Entry 7 in Table 1).

From the above results, it can be concluded that PATMPO **4** polyradical was successfully prepared by the oxidation of PATMP **3** homopolymer and the chemical structure was not altered during the oxidation.

The solubility of PATMPO **4** was tested and it was found that PATMPO **4** polyradical could dissolve in THF, dichloromethane, chloroform and dioxane. In addition, PATMPO **4** polyradical could not dissolve in the commonly used electrolyte, ethylene carbonate and dimethyl carbonate.

#### 3.4. Electrochemical properties of polyradical

PATMPO **4** was used as cathode material for lithium secondary battery to investigate its electrochemical properties. It has been

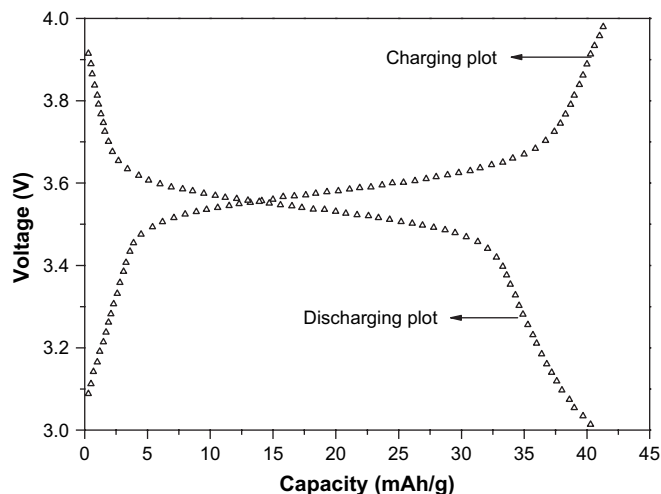


Fig. 6. Charging/discharging curves of Li/PATMPO **4** coin-type cell at a current density of 0.1 A/g in 1 M LiPF<sub>6</sub> EC/DMC (v/v = 1:2) electrolyte.

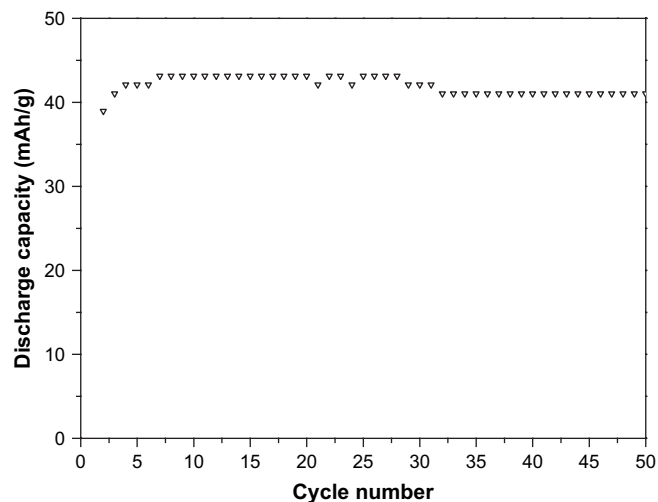


Fig. 7. Cyclic plot of Li/PATMPO **4** coin-type cell at a current density of 0.1 A/g in 1 M LiPF<sub>6</sub> EC/DMC (v/v = 1:2) electrolyte.

reported that stable polymeric nitroxyl radicals possessed excellent redox reversibility and the difference between the anodic ( $E_{a,p} = 3.66$  V vs. Li/Li<sup>+</sup>) and the cathodic ( $E_{c,p} = 3.58$  V vs. Li/Li<sup>+</sup>) peak potentials was much smaller than those of other electroactive organic materials in lithium secondary battery, which led to the fast electrode reaction rate of polyradical during the charging/discharging process [9]. Charging/discharging curves of Li/PATMPO **4** coin-type cell are shown in Fig. 6. The battery was charged and discharged at a constant current density of 0.1 A/g and the voltage ranged between 3.0 and 4.0 V. An obvious plateau can be found in both curves and the voltages of the plateau are 3.6 V (vs. Li/Li<sup>+</sup>) and 3.5 V (vs. Li/Li<sup>+</sup>) for charging and discharging and the maximum charging and discharging capacities were 41.6 and 40.8 mA/g, respectively. Therefore, the coulombic efficiency of the battery was calculated to be as high as 98.1% (40.8/41.6), which showed excellent charging/discharging reversibility.

Fig. 7 shows the cyclic performance of fabricated Li/PATMPO **4** coin-type cell. The charging/discharging process was repeated at a constant current density of 0.1 A/g between 3.0 and 4.0 V vs. Li<sup>+</sup>/Li. After 50 cycles, the discharging capacity of PATMPO **4** just decreased 1.4% compared to the maximum specific capacity, which exhibited excellent stability of PATMPO **4** during the charging/discharging process. All these results suggested that PATMPO polyradical is a promising cathode material for lithium secondary battery.

#### 4. Conclusion

In summary, we have presented the synthesis of polyallene with stable pendant nitroxyl radicals. The radicals were introduced by the oxidation of pendant imino groups of polyallene under mild conditions. PATMPO polyradical was characterized by FT-IR, UV-vis, elemental analysis and ESR.

Electrochemical properties of PATMPO polyradicals were preliminarily investigated and PATMPO showed excellent charging/discharging reversibility and stability, which indicated that PATMPO polyradical is a potential cathode material for lithium secondary battery.

#### Acknowledgement

The authors thank the financial support from Shanghai Nano-Technology Program (0652nm031), Shanghai Rising Star Program

(07QA14066) and the Knowledge Innovation Program of the Chinese Academy of Sciences.

## References

- [1] Miura Y. In: Lahti PM, editor. Magnetic properties of organic material. New York: Dekker; 1999. p. 267.
- [2] Nishide H, Kaneko T. In: Lahti PM, editor. Magnetic properties of organic material. New York: Dekker; 1999. p. 285.
- [3] Semmelhack MF, Chou CS, Cortes DA. *J Am Chem Soc* 1983;105:4492–4.
- [4] Merz A, Bachmann H. *J Am Chem Soc* 1995;117:901–8.
- [5] Semmelhack MF, Schmidt CR, Cortes DA, Chou CS. *J Am Chem Soc* 1984;106:3374–6.
- [6] Yamaguchi M, Miyazawa T, Takata T, Endo T. *Pure Appl Chem* 1990;62:217–22.
- [7] Miyazawa T, Endo T, Okawara M. *J Polym Sci Part A Polym Chem* 1985;23:1527–35.
- [8] Miyazawa T, Endo T. *J Polym Sci Part A Polym Chem* 1985;23:2487–94.
- [9] Nakahara K, Iwasa S, Satoh M, Morioka Y, Iriyama J, Suguro M, et al. *Chem Phys Lett* 2002;359:351–4.
- [10] Suga T, Yoshimura K, Nishide H. *Macromol Symp* 2006;245–246:416–22.
- [11] Nishide H, Iwasa S, Pu Y-J, Suga T, Nakahara K, Satoh M. *Electrochim Acta* 2004;50:827–31.
- [12] Nishide H, Suga T. *Electrochem Soc Interface* 2005;14:32–6.
- [13] Suga T, Konishi H, Nishide H. *Chem Commun* 2007:1730–2.
- [14] Nishide H, Oyaizu K. *Science* 2008;319:737–8.
- [15] Deng LF, Li XH, Xiao LX, Zhang YH. *Acta Polym Sin* 2004;8–12.
- [16] Endo T, Takuma K, Takata T, Hirose C. *Macromolecules* 1993;26:3227–9.
- [17] Kurosaki T, Lee KW, Okawara M. *J Polym Sci Part A Polym Chem* 1972;10:3295–310.
- [18] McGrath MP, Sall ED, Tremont SJ. *Chem Rev* 1995;95:381–98.
- [19] Endo T, Tomita I. *Prog Polym Sci* 1997;22:565–600.
- [20] Børresen S, Crandall JK. *J Org Chem* 1976;41:678–81.
- [21] Fernandes RX, Giri BR, Hippler H, Kachiani C, Striebel F. *J Phys Chem A* 2005;109:1063–70.
- [22] Rozantsev EG, Neiman MB. *Tetrahedron* 1964;20:131–7.
- [23] Chapelet-Letourneux G, Lemaire H, Rassat A. *Bull Soc Chim Fr* 1965:3283–98.